# Observations of the configuration of the high-field vortex lattice in $YBa_2Cu_3O_7$: Dependence upon temperature and angle of applied field

J. S. White, S. P. Brown, E. M. Forgan,* M. Laver, C. J. Bowell, and R. J. Lycett
*School of Physics and Astronomy, The University of Birmingham, Birmingham B15 2TT, United Kingdom*

D. Charalambous
*Cyprus Meteorological Service, CY-1418 Lefkosia, Cyprus*

V. Hinkov
*Max Planck Institut für Festkörperforschung, D-70569 Stuttgart, Germany*

A. Erb
*Walther Meissner Institut BAdW, D-85748 Garching, Germany*

J. Kohlbrecher
*SINQ, Paul Scherrer Institut, CH-5232 Villigen-PSI, Switzerland*

(Received 2 May 2008; revised manuscript received 8 September 2008; published 13 November 2008)

We have mapped out the high-field phase diagram of the vortex lattice in lightly twinned $YBa_2Cu_3O_7$ by employing small-angle neutron scattering. This extends previous measurements [S. P. Brown *et al.*, Phys. Rev. Lett. **92**, 067004 (2004)] in which we reported a transition in local flux-line coordination from distorted triangular to square as a function of field applied parallel to the crystal *c* axis. At high fields, we observe a transition back to triangular coordination with increasing angle between the applied field and *c* axis or with increasing temperature. At lower fields, our results may be interpreted in terms of a field-induced reduction of the basal-plane *a*-*b* anisotropy. Tilting the flux lines away from the *c* axis reduces the pinning by twin planes, changes the orientation of the vortex lattice nearest-neighbor directions, and the transition between square and hexagonal vortex lattices becomes first order.

DOI: 10.1103/PhysRevB.78.174513 PACS number(s): 74.25.Qt, 74.72.Bk, 61.05.fg

## I. INTRODUCTION

The study of vortices in type-II superconductors is a well-established branch of condensed-matter physics. In addition to being fascinating in its own right, it is of fundamental interest because the nature of vortex-vortex interactions arises from the underlying superconducting state: anisotropy in the superconducting gap and nonlocality of the electrodynamics have both been observed to have a profound impact on the coordination and orientation of the vortex lattice.[1–9] Small-angle neutron scattering (SANS) is of importance in structural studies of the vortex lattice (VL) because it is a microscopic probe of the field distribution. As a *bulk* probe, it is unaffected by the systematics of surface-sensitive techniques. Being a diffraction technique, SANS is sensitive to spatial correlations of the vortices, making it highly suited to a diverse range of vortex matter studies including VL melting,[10] flux flow,[11] a range of studies on $YBa_2Cu_3O_{7-\delta}$ that include investigations of twin-plane pinning,[12–19] and studies designed to probe the effect of disorder on the VL.[20–22] In the present context of unconventional VL structures and VL phase transitions, SANS continues to be a fecund source of information and a useful test bed against which to compare theory: recent examples in this area include borocarbides,[23] strontium ruthenate,[24] heavy-fermion materials,[25] and both electron- and hole-doped[26–28] high-$T_c$ materials.

In a previous work[28] a field-induced transition from triangular to square coordination was observed in the VL in $YBa_2Cu_3O_7$ (YBCO), with the field parallel to the crystal *c* axis. This was interpreted as arising from the intrinsic anisotropy of *d*-wave vortex cores, which in a tetragonal *d*-wave superconductor have fourfold symmetry. Such *d*-wave driven VL transitions have been investigated by various phenomenological and first-principles theoretical approaches[29–41] and observations consistent with them have been observed in other systems.[27,42] It should be noted however that in some non-*d*-wave materials (cf. Refs. 8, 9, and 23) there are structural VL phase transitions which may arise from anisotropy of the Fermi surface or of an *s*-wave gap. In YBCO, fourfold or *d*-wave anisotropy is not observable at low inductions ($\lesssim 4$ T). In this field region, the VL assumes a triangular configuration, albeit distorted by the in-plane electronic mass anisotropy. However, at high inductions ($\gtrsim 4$ T), where the basal-plane coherence length $\xi_{ab}$ is no longer insignificant compared with the intervortex spacing, the anisotropy in the vortex-vortex interactions becomes important and the VL is observed to distort continuously into a square lattice at about 11 T.[28]

Here we report further measurements on the same, slightly overdoped, sample as in Ref. 28. We determine the temperature dependence of the transition, with emphasis on the high-field regime where at low temperatures the VL has square coordination. In addition, we detail the dependence of the vortex structures and their phase transitions on the angle between the applied field and the crystal *c* axis for angles in the range $[0°, 30°]$.

 

The remainder of this paper will be divided as follows. In Sec. II the experimental setup will be described. In Sec. III, the field dependence of the results, first presented in Ref. 28, will be reconsidered to provide context for the temperature- and angle-dependent results in Secs. IV and V, respectively. Finally, conclusions will be presented in Sec. VI.

## II. EXPERIMENTAL METHOD

Our experiments were performed on the SANS-I instrument at the Paul Scherrer Institut, Switzerland. Cold neutrons of wavelength $\lambda_n=8$ Å ($\Delta\lambda_n/\lambda_n=10\%$) were collimated over a range of 6–8 m (depending on the desired instrument resolution) and incident on the sample, which was placed inside the variable-temperature insert of a horizontal-field 11 T cryomagnet, with the field applied approximately parallel to the beam. The scattered neutrons were detected with a $^3$He multidetector of $128\times128$ pixels, corresponding to $96\times96$ cm$^2$ placed at a distance equal to the collimation length; the undiffracted beam was terminated by a cadmium beam stop. The reader is referred to Ref. 6 for a general review of the SANS technique as applied to studies of vortices in type-II superconductors.

As detailed in Ref. 28, the sample used herein was a small (approximately 36 mg) high-quality single crystal of $YBa_2Cu_3O_{7-\delta}$, oxygenated close to $\delta=0$.[43,44] A low density of twin planes was present in the sample (spacing $\sim1$ $\mu$m; this is the VL spacing at $B=2$ mT, which is much smaller than the fields applied in this study). These twin planes arise due to a slight orthorhombic distortion which sets in when CuO chains form in the crystal while it is cooled in oxygen from its growth conditions. The twin planes form extended planar defects, which run along the {110} directions, and are capable of pinning the VL and controlling its orientation particularly at low applied fields. This occurs because, in the absence of pinning and at low fields applied parallel to a principal crystal axis, the VL is expected to have a free energy independent of VL orientation.[28,45] The low density of oxygen vacancies (due to the full oxygenation) and the low density of twin planes mean that the VL structures in our sample are likely to be much less affected by vortex pinning than earlier work on optimally doped and more heavily twinned samples.

The sample was initially mounted in the cryostat with the {110} directions horizontal and vertical and with the $c$ axis parallel within 2° of the field applied horizontally. To perform the study of the effects of field direction, the sample holder was rotated about the vertical axis, allowing a range of angles between the applied field and crystal $c$ axis. In all cases, the VL was formed by cooling in the applied field $H$ from above $T_c=86$ K for our sample.[44] Temperature-dependent data were obtained by both cooling to and warming from this field-cooled state. Data were collected by "rocking" (rotating) the cryostat (i.e., sample and field together) through the appropriate small angles ($\approx1°$ for $\approx1-10$ T fields) to satisfy the Bragg condition for diffraction by sets of VL planes. Two orthogonal axes of rotation perpendicular to the beam were available for this purpose, conventionally designated $\omega$ (rotation about the vertical axis) and $\phi$ (rotation about the horizontal axis). Due to the presence of a significant metallurgical signal, in particular at low scattering vector $q$, due to scattering from the sample and cryostat, it was necessary to subtract backgrounds taken above $T_c$ from the data. The experimental technique and data reduction are demonstrated in Fig. 1. In Fig. 1(a), we show raw data taken near the peak of the rocking curve for diffraction spots on the right-hand side of the detector. The main beam is intercepted by a cadmium beam stop and small-angle background scattering from the sample (which includes neutrons reflected from its {100} faces, which are diagonal) is much stronger than the VL signal, so the intensity scale is set to reveal the latter clearly. In Fig. 1(b), background taken above $T_c$ has been subtracted. It will be noted that Poisson noise remains, varying from pixel to pixel of the detector. The resolution of the instrument (mainly due to the finite divergence of the beam, which is set by the collimation distance) is clearly larger than a pixel size, and short-distance intensity variations reflect only noise and not signal. Hence, in the diffraction patterns presented later (but not in any of the fitting), some smoothing has been applied to make the signal more clearly visible. Also Poisson noise around the beam stop where there is no VL signal has been masked. The result of such smoothing and masking is shown in Fig. 1(c). Here, weak signals can also be seen from other spots that did not exactly satisfy the Bragg condition. Finally, to generate complete diffraction patterns (such as those in Figs. 2 and 3), the results from rocking curves over all the spots are summed. The sizes and shapes of VL unit cells were determined from the observed diffraction spot positions—in all cases the determination of the spot positions was made using data from the *peak* of the appropriate rocking curve, so that the position of the spot was not affected by the rocking scan being performed.[46] From the spot positions, the value of the average flux density in the sample could then be calculated by taking one flux quantum $\Phi_0=h/2e$ per unit cell. In all cases, the flux density was experimentally indistinguishable from the applied induction $\mu_0H$, as expected for a superconductor with high Ginzburg-Landau parameter $\kappa$, field cooled in $H\gg H_{c1}$.

## III. FIELD DEPENDENCE

Figure 2(a) shows a diffraction pattern taken at $\mu_0H=2$ T with the field applied parallel to the crystal $c$ axis. The pattern is very similar to that at 1 T shown in Ref. 28. The fourfold symmetry exhibited in such low-field VL diffraction patterns in YBCO is *not* due to the presence of square VLs. Instead, it arises from the addition of the diffraction patterns of four distinct VL domains.[15,16,28,50] The fourfold symmetry in Fig. 2(a) is due to the presence of twin planes, which divide the sample into two different orientations of crystal domains, as illustrated in Fig. 2(f). For each crystal domain, anisotropic London theory[45,48,49] predicts the formation of VL domains that are distorted by the basal-plane penetration-depth anisotropy $\gamma_{ab}\gtrsim1$. This theory, valid for $H_{c1}\ll H\ll H_{c2}$, is therefore quite appropriate for fields of the order of 1–2 T in YBCO which has $\kappa\gg1$. In London theory, anisotropy in the penetration depth $\lambda$ is formulated in terms of

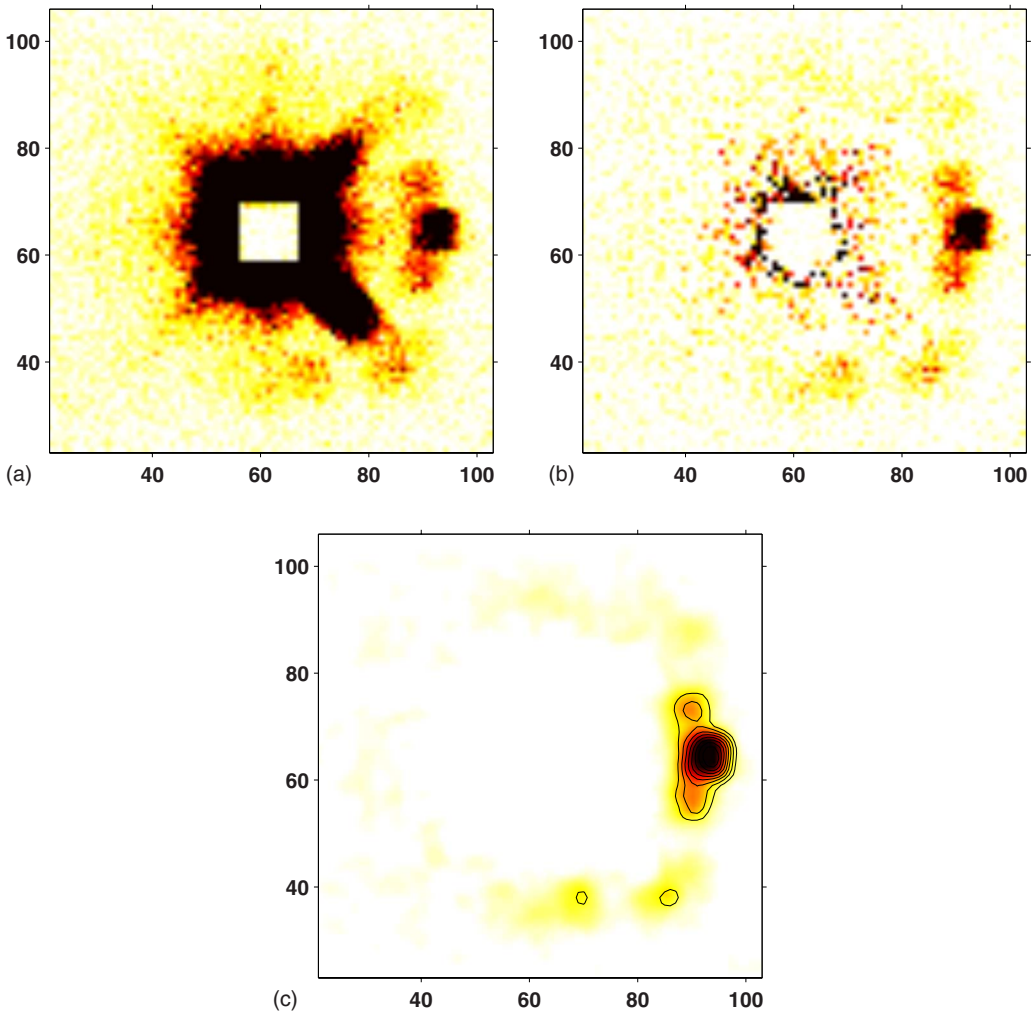


FIG. 1. (Color online) (a) Raw data showing both VL signal and background, taken at 5 K, with 2 T, applied parallel to the crystal *c* axis. The *a* and *b* axes are oriented as shown in Fig. 2(f). The sample and magnet have been rocked in $\omega$ to satisfy the Bragg condition for VL diffraction spots on the right-hand side of the detector. (b) The same data with background subtracted. (c) The data of (b) with masking of Poisson noise near the beam stop, Gaussian smoothing of 3 pixels FWHM, and contours applied. The color scale used has the same range in these three panels and is linear in intensity.

anisotropy of the effective electronic mass; the relation being $\lambda \propto m^{1/2}$. It should be emphasized that in the case of YBCO, the basal-plane effective-mass anisotropy arises from an averaging of the effects of the nearly isotropic $CuO_2$ plane states with the nearly one-dimensional chain states that conduct along the crystal *b* direction. Anisotropy may be introduced into the London equation via the effective-mass tensor, which is second rank. Then for fields applied along one of the principal crystal axes, the distorted VL may be constructed from the undistorted VL by a simple stretch transformation, resulting in a VL with nearest neighbors lying on an ellipse instead of a circle—which is the case for an isotropic effective mass.[45,48,49] From our data at low fields parallel to the *c* axis, we see the ellipse is oriented such that its major and minor axes are parallel to {100}, and we take the axial ratio $\epsilon$ of this observed ellipse to indicate the basal-plane penetration-depth anisotropy, i.e., $\gamma_{ab}=\epsilon$. Within each crystal domain, two VL domains may form, each with the orientation of one set of VL planes pinned to *one* of the twin-plane orientations (horizontal or vertical). This results in four *distorted-triangular* VL domains as illustrated in Fig. 2(f).

As the applied field is increased, a clear change in the coordination of flux lines in each of the domains is observed. Shown in Figs. 2(c)–2(e) are high-field data taken under slightly different conditions than those of Figs. 2(a) and 2(b): the collimation has been relaxed in favor of greater flux. This is desirable because the integrated intensity falls as $1/\sqrt{B}$ from considerations of reciprocal-space geometry alone[51] and even faster if one takes into account finite-core effects, which are ignored in the London theory and lead to a reduction in magnetic contrast in the VL (see Ref. 52 for *s*-wave superconductors). Notwithstanding changes in resolution, a comparison of the high- and low-field data of Fig. 2 reveals a tendency for each of the VL domains to assume a more square configuration at higher fields; the three peaks appearing around each of the {110} directions are closer to each other, and the two peaks arranged either side of the {100} directions have also converged and moved toward the vertex of the square formed by the strong peaks lying directly along

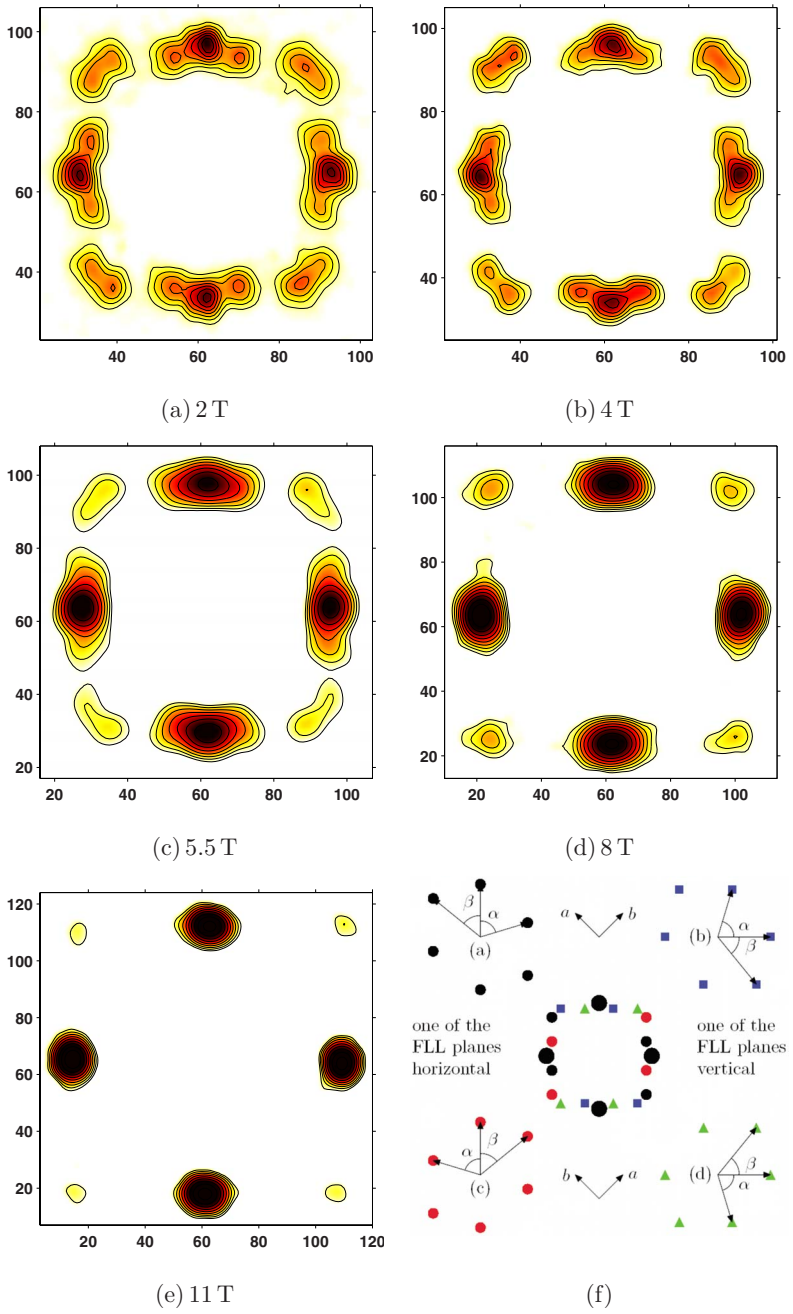


FIG. 2. (Color online) (a)–(e) Diffraction data represented as a sum over rocking curves at 5 K and various fields from 2–11 T applied parallel to the crystal $c$ axis. The orientation of the twinned crystal $a$ and $b$ axes for all these data are shown in (f). In (a) and (b), the sum is over rocking curves in both $\omega$ and $\phi$. The rocks at higher field were carried out with $|\omega|=|\phi|$, thus rocking directly through the weak peaks seen in the corners of the diffraction pattern. These and the weak peaks in the wings of the vertical and horizontal strong peaks are made clearer by the use of a logarithmic intensity scale. The intensity near the horizontal and vertical directions is visible by virtue of the relaxed resolution of our SANS setup and the form of the SANS resolution function (Refs. 46 and 47); for instance, during a rock through the "top-right" region, the resolution will also encompass the peaks at the top and at the right of the diffraction pattern. Backgrounds taken at $T=90$ K$>T_c$ have been subtracted. These data result from four VL domains (two in each crystal domain, each pinned to a different twin-plane orientation). In (f) we illustrate how the VL patterns, seen most clearly in (a) and (b), are formed from the two orientations of crystal anisotropy and two orientations of twin planes present in our sample. The reciprocal-lattice vectors for each VL domain lie on an ellipse which has axial ratio given by the mass anisotropy $\gamma_{ab}$ (Refs. 45, 48, and 49) in the low-field region. The orientation of one of the vectors is known, since one of the VL planes is pinned to a set of twin planes. The magnitude of this reciprocal-lattice vector and the magnitude and direction of the others are then fixed by the shape of the ellipse and flux quantization. Defined in (f) are two angles, $\alpha$ and $\beta$, which characterize the configuration of the VL and its diffraction pattern. Due to the two dimensionality of the VL, the shape and distortion of the *real-space* VL is exactly the same as that of the *reciprocal* lattice, but rotated by 90° about the direction of the field; hence the patterns for each domain may also be viewed as real-space pictures of the vortex arrangement—after addition of a spot at the center of the pattern, corresponding to the position of the masked incident beam.

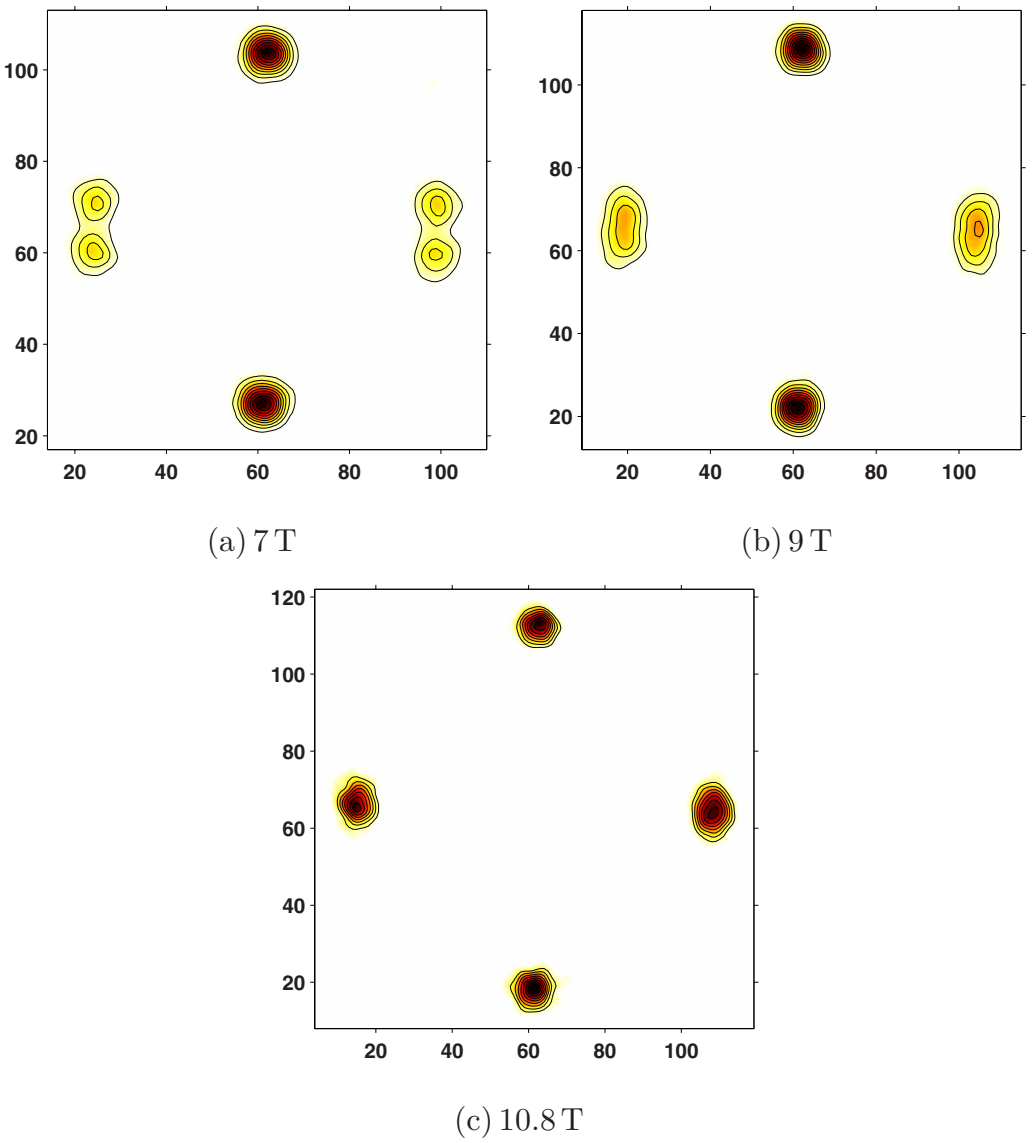


FIG. 3. (Color online) Diffraction patterns taken with fields of 7–10.8 T applied at an angle of 5° to the crystal $c$ axis, yielding only two VL domains therefore providing easier resolution of the horizontal peaks. These data are the sums of rocks in $\omega$ and $\phi$ through angles which satisfy the Bragg condition for peaks to the left/right and top/bottom of the pattern.

{110}. This trend is continued until, within our instrument resolution, only single peaks are observable along the {110} and {100} directions as is shown in the data taken at 11 T [Fig. 2(e)]. These data may be interpreted as arising from a square VL with nearest-neighbor directions along {110}. Such a VL gives rise to weaker spots at higher $q$ along {100} in agreement with our data. Therefore the empirical conclusion from our data is that the VL undergoes a continuous distortion as a function of field from an anisotropic triangular VL to a square VL.[28]

We have undertaken extensive structural studies of the VL in YBCO as a function of field. The twinned nature of our sample makes it difficult to fit the Bragg peaks arising from different domains, particularly at high fields where peaks from different VL domains overlap strongly. To overcome this problem we have repeated these measurements with the field applied at an angle of 5° [in the horizontal, (110) plane] to the crystal $c$ axis. In this situation, the field direction is no longer parallel to the vertical twin planes, although the field still lies within the horizontal twin planes. Hence it is no longer favorable for VL domains to form pinned to the vertical twin planes. Instead, the only VL domains we observe are those pinned to the horizontal twin planes, i.e., those domains giving strong *top and bottom* peaks in Fig. 2. This allows us to resolve better at high fields the peaks close to the horizontal. Although this small angle of rotation is sufficient to remove the influence of the vertical twin planes, it does not appear to affect the structure of the remaining two VL domains nor does it affect the field dependence of the transition. This is not unexpected, since the angle-dependent variations of the twin-plane component of the free energy should vary much more rapidly than components associated with other sources of anisotropy such as ($d$-wave) anisotropy of the order parameter or the effective-mass anisotropy. (The latter varies with the cosine of the angle of rotation and therefore has a negligible effect at 5° rotation.)

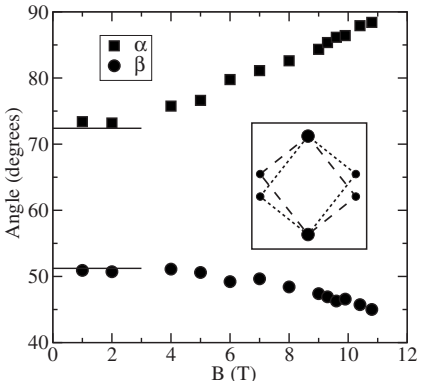


FIG. 4. Variation of the angles $\alpha$ and $\beta$, defined in Fig. 2(f), as a function of field applied at $\leq 5°$ to $c$. The solid lines depict the VL structure predicted by anisotropic London theory using $\gamma_{ab}=1.28$. Inset: an illustration of the orthorhombic distortion of the two (degenerate) VL patterns expected in our sample.

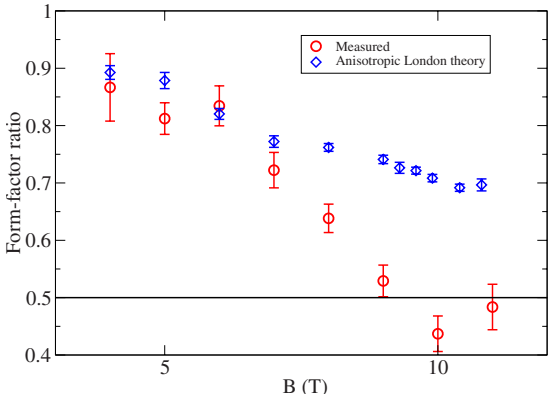


FIG. 5. (Color online) Variation of the estimated ratio of form factors $B_{11}/B_{10}$ versus field (see text for details of the calculation). Also shown is the form-factor ratio expected by anisotropic London theory, using the low-field value of the $a$-$b$ anisotropy ratio, but with the $\boldsymbol{q}$ vectors of the *observed* VL structure. The horizontal line shows the form-factor ratio of 0.5 given by the isotropic London theory applied to a square vortex lattice.

We have used these data to fit the positions of the Bragg peaks and therefore determine the configuration of the VL as a function of field by measuring the two angles, $\alpha$ and $\beta$, as defined in Fig. 2(f). The variation of $\alpha$ and $\beta$ as a function of field is shown in Fig. 4. The two horizontal lines in this figure indicate predicted VL structure using anisotropic London theory calculated for an anisotropy of $\gamma_{ab}=1.28$ with one of the reciprocal-lattice vectors fixed along the {110} direction as controlled by twin-plane pinning. The value of $\gamma_{ab}$ used in this calculation was obtained by fitting to an ellipse the 1 T data reported in Ref. 28. The orientation of the ellipse was taken to be such that the major or minor axes were parallel to {100} (45° to the horizontal or vertical in the diffraction patterns shown).

As the applied field is increased, a continuous deformation of the VL is observed and the values of $\alpha$ and $\beta$ tend to the values expected from an isotropic square VL (90° and 45°, respectively). It appears from the data that this transition is not quite complete even at the highest field available to us (11 T). However, on symmetry grounds one would not expect completely isotropic square VLs to form: truly square VLs would only form in a tetragonal superconductor, whereas the slight ($\approx 1\%$) orthorhombicity of YBCO prohibits this.

In this context, it is of interest to discuss the field dependence of the magnitude of the basal-plane anisotropy $\gamma_{ab}$. The distorted-triangular VL structure at low fields $\lesssim 4$ T is consistent with $\gamma_{ab}\sim 1.28$, but at high fields $\gtrsim 11$ T the VL that is formed is an almost isotropic square. It may be tempting therefore to suggest that the application of large fields tends to suppress the $a$-$b$ anisotropy. However, if one describes the diffraction spots observed at intermediate fields as arising from distorted hexagonal VLs, one obtains a distortion that is *increasing* with field. This apparent paradox arises because the *first-order* spot that defines the longest axis of the ellipse at intermediate fields is destined at high fields to become a *second-order* spot from the square VL. If the anisotropy for an isotropic square VL was defined using this spot, we would obtain $\gamma_{ab}=1.73$. It is therefore clear that the concept of effective-mass anisotropy should be used with caution in this intermediate field range, particularly when some of the diffraction spots are much stronger than others, implying that the latter do not arise from fundamental reciprocal-lattice vectors, but from higher-order reflections. Clearly, at fields $\gtrsim 4$ T, the anisotropic London approach is becoming invalid; further evidence on this matter is given by an examination of the vortex form factor (Fig. 5).

Whatever field-dependent anisotropy is responsible for the continuous transition to a square vortex lattice, it presumably has an impact on the vortex form factor. SANS allows direct measurement of the magnitude of a vortex form factor $B_{hk}$ because $I_{hk}$, the intensity of the $(h,k)$ Bragg reflection integrated over the rocking curve,[51] is proportional to $|B_{hk}|^2$. However, such measurements are prohibitively time consuming, particularly for weak second-order reflections and so were not performed. Nevertheless, the integrated intensity of a Bragg reflection may be estimated, to within a constant factor proportional to the rocking curve width, from its *peak* intensity. The usefulness of this estimate relies on the equality of rocking curve widths belonging to different reflections and their constancy as a function of field. Given the shearlike transformation observed, it is unlikely that the rocking curve widths will remain constant as a function of field. Moreover, the instrument setup, i.e., resolution, was varied (to obtain maximum intensity) as a function of field, thus the rocking curve widths will certainly not remain constant. The latter systematic effect, and to a certain extent the former one too (if the changes in rocking curve width are the same for all reflections), may be removed by calculating the *ratio* of peak intensities of Bragg reflections as a function of field.

The intensities of the strong doubly-degenerate reflections lying along the vertical crystal {110} direction and the weak reflections lying near the crystal {100} directions have been estimated by *fitting* two-dimensional Gaussians to the spots observed at the peaks of the rocking curves in the data with $\boldsymbol{H}$ parallel to the $c$ axis. Ordinarily, one would prefer simply to sum the detector counts, but this would give rise to systematic errors since counts from nearby spots often overlap

on the detector. At high fields, where the vortex lattice is almost square, the fitting routine was unable to resolve closely spaced diffraction peaks. Then it was necessary to fit a single Gaussian to a pair of spots and divide the estimated intensity by two to account for the degeneracy.

In Fig. 5 is shown the field dependence of the ratio of form factors $|B_{11}/B_{10}|$ obtained by the method described above. [The conversion from intensity to form factor has been performed using the expression[51] $|B_{hk}| \propto \sqrt{I_{\boldsymbol{G}}|\boldsymbol{G}|}$, where $\boldsymbol{G}$ is the $(h,k)$ reciprocal-lattice vector.] Also shown in the figure is the form-factor ratio for an isotropic square London vortex lattice (0.5) and the prediction of anisotropic London theory given the measured penetration-depth anisotropy (assumed field independent) and the observed vortex lattice structure (see Fig. 4). Both of these ratios may be deduced from the expression for the form factor in the presence of basal-plane anisotropy, which can be calculated from London theory[18,53]

$$B_{hk} = \frac{\mu_0 H}{1 + \lambda_L^2 (G_x^2 m_{yy} + G_y^2 m_{xx})}. \quad (1)$$

In this expression, $\lambda_L^2$ is the geometric mean penetration depth, the 1 in the denominator may be disregarded for $H > H_{c1}$, and the ratio of the normalized effective masses $m_{yy}$ and $m_{xx}$ is set to unity for the isotropic square vortex lattice or $\gamma_{ab}^2$ for the anisotropic London calculation.

Figure 5 shows explicitly that the diminished intensity of the corner spots observed at high fields is not simply a consequence of the larger ratio of $G_{11}/G_{10}$, but that there is an additional effect on the vortex form factor beyond what the London theory predicts for the measured *low-field* anisotropy. The data do seem to tend at high fields toward the predictions for an *isotropic* square vortex lattice. However, while this may imply that vortices in YBCO at high fields have a more isotropic London-type form factor, the apparent field dependence of the anisotropy highlights that the vortex lattice is *not* purely London-type in this regime.

In the broadest sense, the distorted triangular to square VL transition may be classified in terms of the increasing nonlocality with increasing field. This nonlocality, not present in the standard London and Ginzburg-Landau theories, may nevertheless be introduced to account for VL phase transitions related to the one presented here. In Ginzburg-Landau theory, the effects of increasing nonlocality may be modeled by inserting higher-order gradient terms that couple to some underlying anisotropy. Such higher-order terms are present in the *d*-wave extensions to the Ginzburg-Landau theory.[29–33,37] These terms may give rise to a free-energy minimum for a square VL rather than the conventional triangular one. Likewise, if London theory is amended with nonlocal corrections[5] (amounting to a dispersive relationship between the Fourier coefficients of the current density and vector potential, arising from their integral relationship in real space) then unconventional VLs may also arise. It should also be noted that the effects of a *d*-wave variation of the gap around the Fermi surface may also be approximately represented by a nonlocal London theory.[54] In any of these cases, the higher-order terms give a quite different kind of anisotropy compared to the local theories and the resulting VL distortions may not be just "scaled away." As a consequence, not only does nonlocality favor a particular VL coordination, but it also favors a particular orientation.

Although the phenomenological London and Ginzburg-Landau theories are intuitively appealing, neither may be applied directly to the transition observed here. In the simplest form of nonlocal London theory such as in Ref. 5 it is assumed a *uniform* (*s*-wave) superconducting gap, which is certainly not the case in YBCO, although the theory has been applied to the borocarbides, which also now appear to have nonuniform gaps. A *d*-wave version of nonlocal London theory[54] also appears not to be appropriate since its predictions are quite different from what we observe. On the other hand, we cannot apply *d*-wave Ginzburg-Landau theory,[29–33,37] which is only accurately applicable when the order parameter is small, and our data were taken at low temperatures and also not near $H_{c2}$.

Numerical calculations based on the quasiclassical Eilenberger theory[34,35,39,55] are potentially useful for analyzing our data since they are, in principle, valid at arbitrary temperatures and fields, although obtaining solutions is numerically intensive. The two essential ingredients to this theory that may give rise to a square VL are Fermi-surface anisotropy and anisotropy of the order parameter. In YBCO there is an intrinsic *d*-wave superconducting gap anisotropy, which is such that there are nodes close to {110} and antinodes along {100}. This anisotropy affects the field profile of each vortex, giving it a fourfold symmetry that is particularly pronounced in the region of the vortex core.[39] We note that *magnetic* interactions are not primarily responsible for the appearance of the square VL because the field profile rapidly becomes more isotropic at distances $\gtrsim \xi$ from the core. Instead, these theories indicate that square VLs are caused by the presence of low-energy quasiparticle states extending well away from the vortex core along the nodal directions. Tunneling of quasiparticles between vortex cores is enhanced if nearest neighbors align along {110}, resulting in an additional component to the vortex-vortex interaction energy. At low inductions (large intervortex spacings), this is not sufficient to result in a square lattice, but as the field is increased and the vortices become more closely spaced, the propensity for a square VL increases.

Fermi-surface anisotropy also couples the crystal lattice to the VL. Even in local London theory, electronic anisotropy distorts the VL via the effective-mass tensor. However, in this theory the local relationship between current density and vector potential only distorts the triangular VL expected for an isotropic situation. Electronic anisotropy can, however, directly affect the coordination of the VL when nonlocal corrections are added to the London theory.[5] In YBCO the principal Fermi surface is associated with the $CuO_2$ planes and is a holelike surface centered on the Brillouin-zone corner,[56,57] with an approximately cylindrical shape. This is slightly distorted so that the Fermi velocity is larger along $k_x$ and $k_y$ than along the {110} directions. Comparing with nonlocal London theory,[5] we note that the Fermi-surface anisotropy for YBCO is of such a sign that it would give rise to the same qualitative effect on the structure of the VL as would order-parameter anisotropy due to the *d*-wave nodes. Therefore,

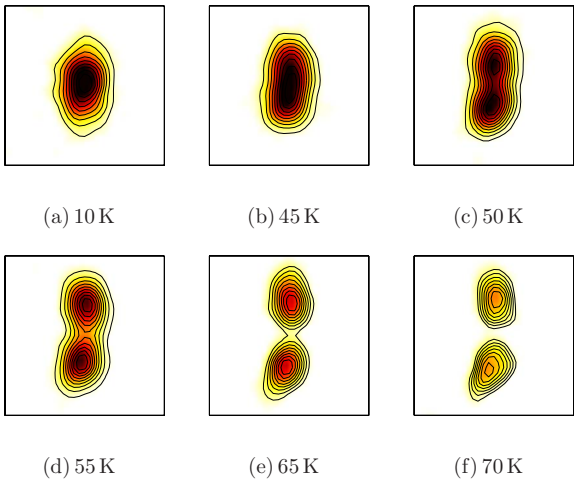


FIG. 6. (Color online) The diffraction peaks on the right-hand side of the detector at an induction of 10 T applied at 5° to the crystal $c$ axis, at selected temperatures in the range 10–70 K. Increasing temperature leads to a splitting of the spots, which is a signature of a return to a distorted-triangular lattice at high temperatures.

from our data alone, we are unable to determine whether the field-induced VL structural transition we observe has its origins in the anisotropy of the Fermi surface or the anisotropy of the order parameter. In any case, such a sharp distinction between these two effects does not reflect the physics since both anisotropies originate from the underlying crystal structure and both can be approximated by a nonlocal London theory.[5,54] Moreover, in the quasiclassical theory[41] the order-parameter anisotropy and the angle-resolved density of states enter symmetrically in the expression for the free energy.

## IV. TEMPERATURE DEPENDENCE

We have performed temperature scans at various applied fields to establish the phase diagram of VL structures in our YBCO sample. As before, to reduce the complications due to the twinned nature of our sample, these measurements were carried out with the field applied at 5° to the crystal $c$ axis. In Fig. 6 we show a selection of our measurements taken over the temperature range 10–70 K. Vortex lattices were formed by cooling into and warming from a field-cooled state, but no hysteresis was observed. In Fig. 6 we focus on the diffraction peaks on the right-hand side of the detector (cf. Fig. 3). We have seen that these peaks transform from a doublet at low fields to a singlet at high fields. The sequence of diffraction patterns in Fig. 6 shows that with increasing temperature there is a clear tendency to change back to the distorted-triangular VL observed at low fields. The absence of hysteresis and the smooth variation of the spot spacing with temperature show that the changes in VL structure are not due to temperature dependence of twin-plane pinning (which in any case has been made inoperative for the spots near the horizontal by the 5° rotation of the field). This provides further confirmation of the intrinsic nature of the transition to a square VL at high fields.

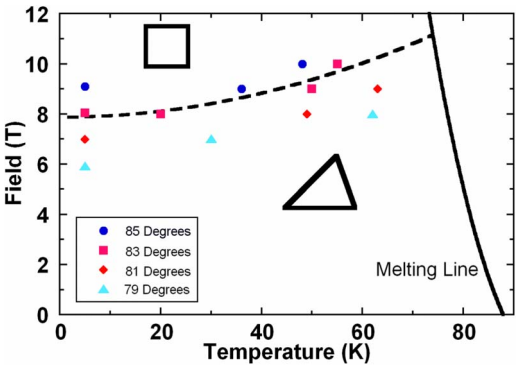


FIG. 7. (Color online) Schematic indication of the VL coordination in our YBCO sample. The VL melting line from Ref. 44 is also shown. Since the transition is continuous, the dashed line separating the square and triangular phases has been drawn where the angle (83°) between the two reciprocal-lattice vectors is halfway between the square and distorted-triangular limits. The temperature errors in the points used to draw this line are approximately equal to the size of the symbols.

Even with these temperature-dependent data, it remains difficult to distinguish between the two candidate origins of the square vortex lattice, namely, order-parameter anisotropy and Fermi-surface anisotropy. In both cases, the continuous transition observed with increasing temperature may be understood in terms of thermal fluctuations "smearing out" the anisotropy generating the square VL. In the $d$-wave order-parameter scenario, the distribution of quasiparticles becomes more isotropic with increasing temperature as the difference in the superconducting gap between nodes and antinodes becomes less important compared with $k_BT$. This in turn reduces the free energy gained by quasiparticle tunneling between vortices with nearest neighbors along {110}, which is the origin of the appearance of a square lattice in a $d_{x^2-y^2}$ superconductor. In this context, we note that the $d$-wave nonlocal London theory[54] gives vortex lattice structures that become increasingly isotropic with increasing temperature. On the other hand, from a Ginzburg-Landau viewpoint, high temperatures reduce the magnitude of the order parameter, which reduces the influence of the nonlinear terms and thus the free-energy density tends toward an $s$-wave type expression. Thermal fluctuations have a similar effect on the anisotropy within nonlocal $s$-wave London theory.[5] At constant induction and in the clean limit, the nonlocal term decreases by a factor of roughly 2 between low temperatures and $T_c$.

In Fig. 7 we have constructed a schematic diagram for the VL structures in our YBCO sample from our measurements as a function of temperature at various applied fields. The line representing the continuous transition between square and distorted-triangular phases is drawn where the angle between reciprocal-lattice vectors is at the midpoint of its variation between the two phases. This line is fairly flat at low temperatures, but is observed to curve upwards with increasing temperature. This is consistent with the increasing role played by thermal fluctuations in smearing out the anisotropy.

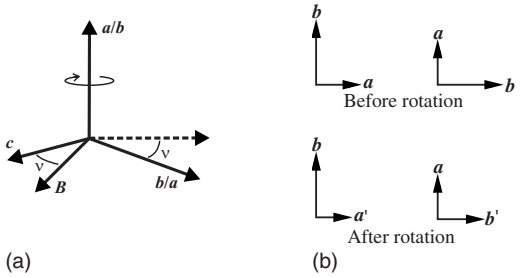


FIG. 8. Schematics showing (a) the direction of rotation, $\nu$, of the $c$ axis away from the field for our data presented in Sec. V and in (b) the effect of this rotation on the effective mass in the plane perpendicular to the vortex direction, where shorter lines represent larger effective masses. Since $m_c \gg m_a \approx m_b$, rotation as depicted in (a) increases the effective mass in the horizontal direction. Therefore crystal domains with $b$ vertical will become more anisotropic, while those with $a$ vertical will become less anisotropic.

## V. DEPENDENCE ON APPLIED FIELD ANGLE

By applying the magnetic field at an angle to the crystal $c$ axis we were able to reduce greatly the influence of twin-plane pinning and also to study the influence of the crystal anisotropy on the triangular to square transition. For such studies we chose a rotation plane such that *both* sets of twin planes are rotated away from the field direction. Therefore, we do not expect the twin planes to exert a strong influence over the orientation of any VL domains present. As illustrated in Fig. 8(a), the orientation of the crystal is such that the applied field and the $c$ axis are in the horizontal plane, one of the {100} directions is vertical, and the other is in the horizontal plane. Note that this rotation plane is not the same as that used in Secs. III and IV where the applied field was rotated away from the $c$ axis in a direction *parallel* to one set of twin planes but at 5° from the other set, and where we found that 5° was sufficient to depin the vortices from the second set of twin planes. The expected suppression of twin-plane pinning using the rotation plane illustrated in Fig. 8(a) is confirmed by the low-field (5 T) VL diffraction pattern shown in Fig. 9(a) where there is a conspicuous absence of the *strong* Bragg peaks in the directions of the twin planes, unlike the data with $\boldsymbol{B}$ parallel to the $c$ axis (Fig. 2).

The principal peaks in Fig. 9(a) belong to two triangular-coordinated VLs each of which gives rise to a slightly distorted hexagon containing a pair of spots oriented either horizontally or vertically in the diffraction pattern. In our twinned sample, the vertical direction corresponds to the directions of either $a$ and $b$ axes of the two crystal domains arising from the twinned nature of our sample; the horizontal direction is the projection in the plane perpendicular to the applied field of the respective $b$ and $a$ directions of each crystal domain. The observation of the two VL domains in roughly equal proportions can be ascribed to the twinned nature of our sample. For brevity, these domains will hereafter be referred to as the "horizontal triangular domain" (HTD) and the "vertical triangular domain" (VTD), respectively. The HTD (VTD) domains are illustrated by the dashed blue (solid black) hexagons in Fig. 9(a). The VTD appears to be oriented as expected from anisotropic London theory,[45,58] but the HTD is not. It is likely that the VL orientation is in fact coupled to the crystal structure of the domain in which it lies. We may deduce which VL belongs to which crystal domain by measuring their distortions, which should reflect the basal-plane anisotropy at low fields. The positions of the peaks of each VL domain yield the angles between the reciprocal-lattice vectors and thus the axial ratio $\epsilon$ of the ellipse upon which the diffraction spots lie. For the HTD, these are 54.2(6)° and 63.0(5)°, giving $\epsilon_{\mathrm{HTD}}=1.14(2)$, stretched in the vertical direction. For the VTD, the corresponding values are 50.3(6)° and 64.9(3)°, with an axial ratio of $\epsilon_{\mathrm{VTD}}=1.229(6)$, but stretched in the horizontal direction. We therefore deduce that the HTD is formed in the domains with the $a$ axis vertical and the VTD is formed where the $b$ axis is vertical. Bearing in mind the 90° relative orientation of real and reciprocal vortex lattices, this implies that both domains have VL nearest-neighbor directions aligned with the crystal $a$ axis. This is also the VL orientation observed at 3.8 T in a partially detwinned crystal with the field rotated from the $c$ axis.[17]

However, it should be noted that the distortions of both VTD and HTD are significantly smaller than that due to basal-plane anisotropy seen at low fields $\lesssim 4$ T with $\boldsymbol{H}$ parallel to the $c$ axis, where $\epsilon=1.28(1)$ [Fig. 2(a)]. This suggests that when the hexagonal VL is no longer constrained in orientation by twin-plane pinning, a reduced $a$-$b$ anisotropy at higher fields $\approx 5$ T is revealed. At these fields, we expect that the anisotropic London theory is no longer quantitatively applicable, but qualitatively it does predict that the rotation of the field from the $c$ axis leads to the observed larger VL distortion in the VTD domain that has $b$ vertical, as illustrated in Fig. 8(b). Quantitatively, the anisotropic London theory predicts a negligible change in the VL distortion for small rotations $\nu$ of applied field away from the $c$ axis, as is clear from the relation[48,49]

$$\epsilon(\nu) = \epsilon(0)[\cos^2(\nu) + (m_{ab}/m_c)\sin^2(\nu)]^{1/2} \qquad (2)$$

for uniaxial superconductors. Thus one would expect the axial ratios of the ellipses fitting the HTD and VTD domains to be equal within a few percent [$\epsilon(10°)/\epsilon(0)=0.99$ from Eq. (2)]. That this is not the case, again, indicates anisotropic London theory is no longer strictly applicable in this field range.

Although the diffraction pattern shown in Fig. 9(a) does not have strong scattering along the {110} directions, *weak* peaks are in fact present along these directions in the diffraction pattern. Their positions on the diffraction pattern are not inconsistent with the vortices being correlated with the twin planes. Due to overlap with the strong peaks, it was not possible to fit accurately the positions of the weak peaks, thus making it impossible to determine unambiguously the associated vortex structure. What can be said about the weak peaks is that their $q$ value, 32.6(2) mÅ$^{-1}$, is too large for scattering from a square arrangement of vortices (30.9 mÅ$^{-1}$) and too small for scattering from an isotropic triangular structure (33.2 mÅ$^{-1}$). The most probable explanation for the weak spots is that they belong to four distorted-triangular VLs, each with one lattice vector along {110}, similar to those observed at low fields with the field

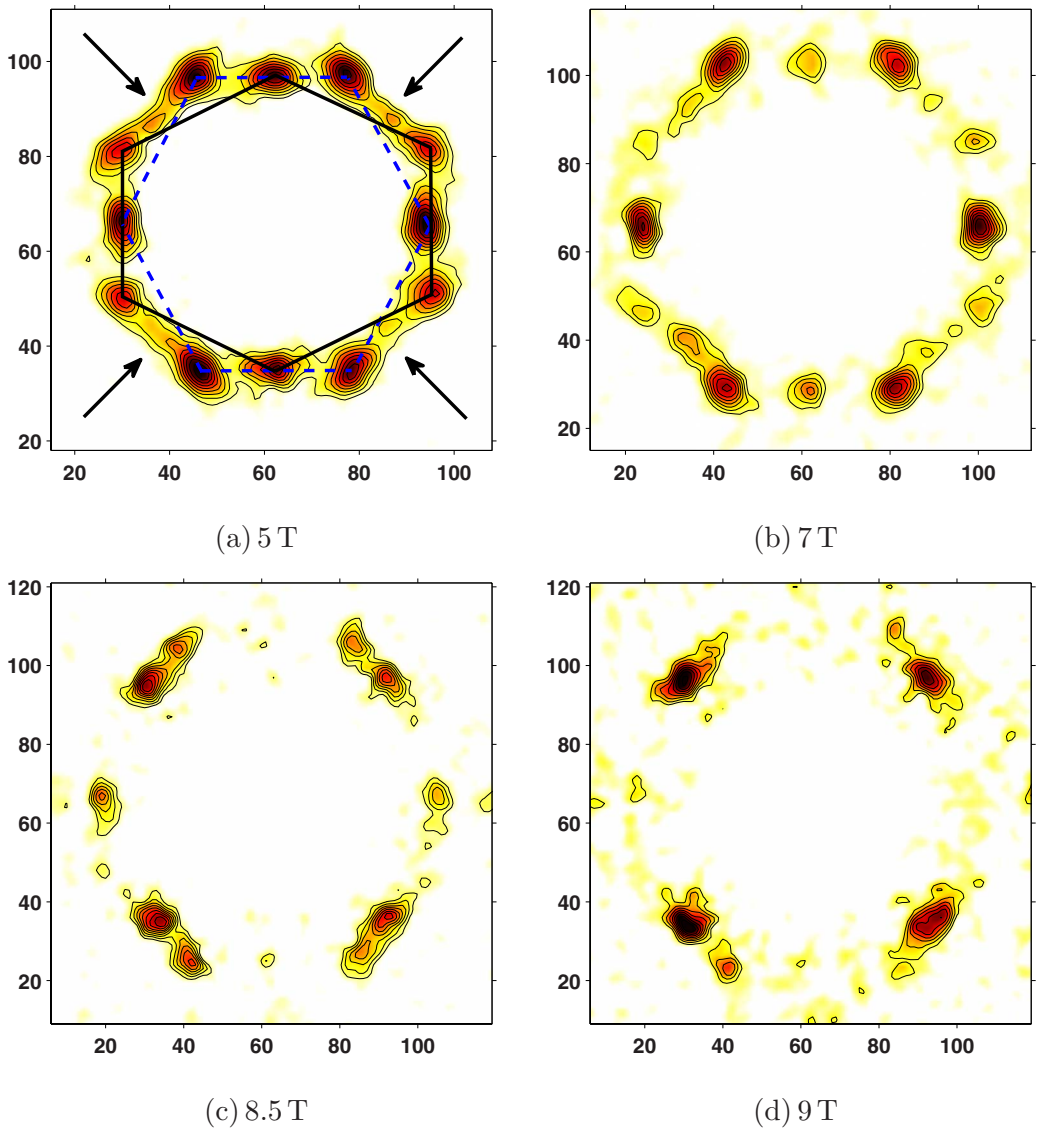


FIG. 9. (Color online) Field dependence of the VL domains present with the field applied at $\nu=10°$ to the $c$ axis in the rotation plane illustrated in Fig. 8(a). Thus the $a/b$ axes are vertical in the figures and the field direction was at $(10/\sqrt{2})°$ to the twin planes. All data were taken at 5 K. The pattern in (a) is due to at least two distinguishable VL domains. The diffraction pattern arising from one of these domains, indicated by the dashed blue lines, includes two horizontal spots and the VL is referred to as the "HTD" in the text. The other, indicated by the solid black lines, includes two vertical spots, and the VL is referred to as the "VTD." The arrows, which lie parallel to the projection on the detector of the sample {110} directions, indicate the positions at which strong scattering would be observed with the field applied parallel to the sample $c$ axis (cf. Fig. 2); in the present arrangement, only weak scattering is observed at these points.

parallel to $c$. We note the weak spots cannot originate from flux lines running *within* the twin planes because such VLs would lie at the wrong angle to cause Bragg diffraction of neutrons. Thus the mechanism responsible for orienting the vortices cannot simply be direct pinning by the twin planes. Perhaps, as suggested in Ref. 14, the vortices are pinned to the *intersections* of the twin planes with the $CuO_2$ planes. Alternatively, the nodes in the $d$-wave order parameter may be responsible for the observed alignment: within quasiclassical $d$-wave theory[39] the free energy of a triangular VL aligned with {110} is very close to that of a similarly coordinated VL aligned along the crystal axes.

Returning to the strong diffraction peaks of Fig. 9, it is of interest to note that there is rather little variation in the distortion of the VTD and HTD as a function of field. However, as the applied field is increased a substantial change in occupation of the VL domains is observed. At 7 T the VTD is visibly weaker compared to the HTD and the peaks observed along the diagonals appear more intense. This is the highest field at which the VTD was observed and here the angles of its reciprocal lattice are $[51(1)°, 65(1)°]$, which is rather similar to $[50.3(3)°, 64.9(3)°]$ measured at 5 T. At 8.5 T the VTD has disappeared and the peaks along the diagonals are now of comparable intensity to those of the HTD. This was the highest field for which the structure of the HTD could be determined. As with the VTD, the angles of the reciprocal lattice, $[58.3(5)°, 61.0(5)°]$, are not too different from their values at 5 T, $[54.2(6)°, 63.0(5)°]$. At 9 T even the HTD is

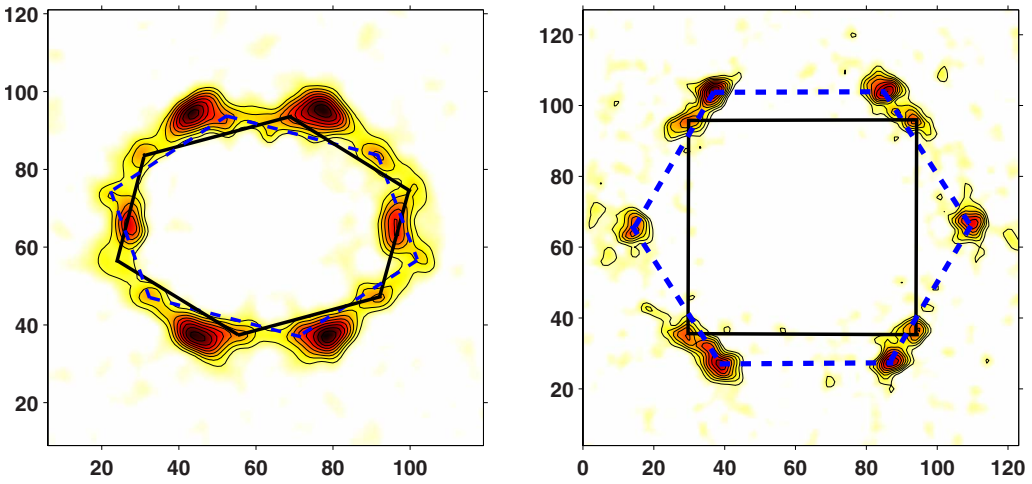


(a) 5 T (b) 9 T

FIG. 10. (Color online) Diffraction pattern taken at 5 K with the crystal $c$ axis rotated by $\gamma=30°$ away from the direction of the applied field of (a) 5 T and (b) 9 T. In (a) the HTD observed in the 10° data [Fig. 9(a)] is clearly visible, but the VTD is absent. In its place are two distorted-triangular VLs whose diffraction patterns are indicated by dashed blue and solid black lines. In (b) the HTD is still present but in addition there is an approximately square VL domain.

barely discernible and the major part of the observed scattered intensity occurs at the peaks along the diagonals. These peaks are the first-order peaks of *square* VL domains aligned approximately along the {110} directions. Therefore, at high fields the observed VL structure is very similar to that seen with $\boldsymbol{B}$ applied parallel to the crystal $c$ axis.

The coexistence over a wide range of fields of the HTD and VTD with the square VL domains aligned with {110} suggests that they are separated by a first-order transition occurring below the irreversibility temperature, which can cause vortex structures to be frozen in. To check this we have performed temperature scans at 8.5 T to study the temperature dependence of the structure and relative occupied volumes of the HTD and the square VL domains. The VLs were prepared by field cooling the sample down to 20 K. Measurements were taken at intervals of 10 up to 70 K, where the scattered intensity was immeasurably small. Measurements were then taken going down in temperature to 50 K. No change in the *structures* of either the HTD or the square domain was observed, while the ratio of these domains' scattered *intensities* exhibited hysteretic behavior. This is consistent with a first-order transition between two distinct structures, with the transition between them hindered by pinning. At 50 K, the ratio of the scattered intensity of the HTD to that of the square domain was 0.6(1) when increasing the temperature but 0.8(1) when decreasing the temperature. This suggests that the HTD structure is frozen in at a temperature above that of a first-order transition to the {110}-oriented square structure.

To elucidate further the dependence of the VL structure on the applied field angle we have obtained data with the field applied 30° to the $c$ axis (Fig. 10). The data at an applied field of 5 T [Fig. 10(a)] show that the HTD is still present, albeit slightly more isotropic [with measured lattice angles of 59.4(2)° and 61.2(4)°] than when the field was applied at 10°. Qualitatively, this is exactly what is expected for the HTD domain since the rotation of the $b$ axis out of the plane perpendicular to the applied field would tend to make the effective mass more isotropic. Using Eq. (2), an isotropic VL would be expected for a rotation of 38° in our sample, though we emphasize that anisotropic London theory does not contain the higher-order terms necessary to explain the vortex structures observed and thus these remarks represent at best only a qualitative understanding of the evolution of the HTD with applied field angle.

It can be seen from Fig. 10(a) that the VTD is not present. Presumably this is because the VTD only forms when the field is applied close to perpendicular to the crystal $a$ axis in this crystal domain, which in the present situation has been rotated away by 30°. Instead two triangular VLs form, which are very distorted owing to the rotation which "reinforces" the $a$-$b$ anisotropy in this crystal domain [Fig. 8(b)]. The correctness of these structures has been tested by measuring the $\boldsymbol{q}$ vectors of the Bragg peaks and establishing that the proposed lattices obey flux quantization; it was not possible to confirm that the supposed structures form Bravais lattices because the Bragg peaks lying close to the strong spots in Fig. 8(b) are too obscured to get reliable fits of their positions. The orientation of these two VLs is quite unusual: both form with nearest-neighbor directions at 15° to the vertical $a/b$ direction, which does not correspond to any special crystal direction. The mechanism controlling the configuration of these VLs is at present a mystery, but quite similar structures have been observed in a different sample of fully oxygenated YBCO at a lower field of 0.8 T.[14] There it was claimed that the orientation was consistent with vortex alignment along the intersections of the twin planes with the basal plane. That explanation does *not* fit our data: for a rotation of $\gamma=30°$ the twin-plane-correlated nearest-neighbor direction would be 41° to the vertical rotation axis, which is significantly different from the 33° that we observe.

At 9 T applied 30° to the $c$ axis [Fig. 10(b)], the two unusual distorted-triangular VLs that exist at lower fields

[Fig. 10(a)] have been replaced by single spots along the diagonals. These correspond to a square VL, whose {1,1} peaks are just visible at the very edges of the detector in Fig. 10(b). Also present is the HTD, though we note its diffraction peaks are stronger relative to those of the square VL than was seen with 9 T applied at 10° to *c* [Fig. 9(d)]. Thus increasing the angle of applied field away from parallel to the *c* axis appears to suppress the VL transition to square, as would be expected if the anisotropy that induces the square VL manifests in the basal plane.

## VI. CONCLUSIONS

In the present work, we have demonstrated the overall theme that the VL in $YBa_2Cu_3O_7$ changes from hexagonal coordination at low fields to essentially square at high fields. However, the detailed VL alignment and coordination in lightly twinned YBCO are affected by a large number of factors: the alignment of some of the VL Bragg planes by twin planes, the *d*-wave nature of the pairing, the crystal basal-plane anisotropy related to the orthorhombic crystal structure, the magnetic-field value and direction, and the temperature. When VLs are formed by a field applied parallel to the crystal *c* direction, then vortex lines can lie within twin planes and the effect of alignment of the VLs by twin planes is maximized. At low fields, the coordination of the vortices is distorted from regular hexagonal by the *a*-*b* crystal anisotropy, but the *alignment* of the hexagonal lattices is determined by the locking of one of the VL planes to twin planes. In this geometry, it is not possible to be certain whether the high-field square coordination and the alignment of VL nearest neighbors along {110} directions arise from twin-plane pinning or *d*-wave effects.

However, if the field is applied in a direction rotated from *c* by ~5° toward a [110] direction, the aligning effect of one set of twin planes is essentially removed, although the applied field still lies within the other set of twin planes and their aligning effect remains. Rotation in this direction has the advantage that both crystal domains in the twinned sample remain in the same relative orientation with the applied field and the reduction in the number of different VL domains allows a detailed investigation of the continuous change of VL geometry with field and temperature. When the temperature is raised, we find that the transition out of the distorted hexagonal structure occurs at a higher field. This is consistent with the VL transition being due to *d*-wave effects, in that the anisotropy in the *d*-wave gap will become relatively less important compared with $k_BT$ as the temperature is raised. However, we cannot rule out the influence of "nonlocal" effects arising from Fermi-surface anisotropy. This is because nonlocality would give the same high-field VL orientation as expected from *d*-wave theory and also because nonlocal effects also become somewhat weaker at higher temperatures.

We have also investigated the effect of rotating the field direction away from *c* toward a [100] direction. This means that the vortices are not parallel to either set of twin planes. As expected, this greatly reduces the aligning effect of both sets of twin planes. However, this direction of rotation means that the two crystal domains are in a different relative orientation to the field (one has been rotated about *a* and the other about *b*). At a small rotation angle of ~10°, the VLs are not aligned by twin planes nor are they in the orientation expected from anisotropic London theory; instead they are aligned with the *a* and *b* crystal axes. In this case, we observe reduction of *a*-*b* anisotropy at fields ≈5 T, as indicated by a change in the distortions of the hexagonal VLs. At somewhat higher fields, a transition to a nearly square VL occurs. This transition differs in two respects from that observed with $\boldsymbol{H}$ parallel to *c*: it begins at a lower field and it is *first order*, as evidenced by the coexistence of the low- and high-field VLs. At still larger angles of tilt, there is a tendency to suppress the transition to the square VL, as would be expected for a transition driven by the *d*-wave symmetry in the basal plane. It would be of great interest to investigate the VL structures in a fully detwinned sample of YBCO in order to fully disentangle the effects of field direction and the removal of twin-plane pinning.

## ACKNOWLEDGMENTS

This work is based on experiments performed at the Swiss spallation neutron source SINQ, Paul Scherrer Institute, Villigen, Switzerland. We acknowledge financial support from the Engineering and Physical Sciences Research Council of the U.K., H. Keller (University of Zürich), the Institut Laue-Langevin, the University of Birmingham, and the European Commission under the 6th Framework Programme through the Key Action: Strengthening the European Research Area, Research Infrastructures under Contract No. RII3-CT-2003-505925.

*e.m.forgan@bham.ac.uk

[1] T. Koyama, M. Tachiki, H. Matsumoto, and H. Umezawa, Phys. Rev. B **20**, 918 (1979).

[2] D. K. Christen, H. R. Kerchner, S. T. Sekula, and P. Thorel, Phys. Rev. B **21**, 102 (1980).

[3] Y. De Wilde, M. Iavarone, U. Welp, V. Metlushko, A. E. Koshelev, I. Aranson, G. W. Crabtree, and P. C. Canfield, Phys. Rev. Lett. **78**, 4273 (1997).

[4] V. G. Kogan, P. Miranović, L. Dobrosavljević-Grujić, W. E. Pickett, and D. K. Christen, Phys. Rev. Lett. **79**, 741 (1997).

[5] V. G. Kogan, M. Bullock, B. Harmon, P. Miranović, L. Dobrosavljević-Grujić, P. L. Gammel, and D. J. Bishop, Phys. Rev. B **55**, R8693 (1997).

[6] E. M. Forgan, *Neutron Scattering in Layered Copper-Oxide Superconductors* (Kluwer, Dordrecht, 1998).

[7] M. R. Eskildsen, A. B. Abrahamsen, D. López, P. L. Gammel, D. J. Bishop, N. H. Andersen, K. Mortensen, and P. C. Canfield, Phys. Rev. Lett. **86**, 320 (2001).

[8] M. Yethiraj, D. K. Christen, A. A. Gapud, D. McK. Paul, S. J. Crowe, C. D. Dewhurst, R. Cubitt, L. Porcar, and A. Gurevich, Phys. Rev. B **72**, 060504(R) (2005).
[9] M. Laver *et al.*, Phys. Rev. Lett. **96**, 167002 (2006).
[10] R. Cubitt *et al.*, Nature (London) **365**, 407 (1993).
[11] D. Charalambous *et al.*, Phys. Rev. B **66**, 054506 (2002).
[12] E. M. Forgan, D. McK. Paul, H. A. Mook, P. A. Timmins, H. Keller, S. Sutton, and J. S. Abell, Nature (London) **343**, 735 (1990).
[13] M. Yethiraj, H. A. Mook, G. D. Wignall, R. Cubitt, E. M. Forgan, D. M. Paul, and T. Armstrong, Phys. Rev. Lett. **70**, 857 (1993).
[14] M. Yethiraj, H. A. Mook, G. D. Wignall, R. Cubitt, E. M. Forgan, S. L. Lee, D. M. Paul, and T. Armstrong, Phys. Rev. Lett. **71**, 3019 (1993).
[15] B. Keimer, W. Y. Shih, R. W. Erwin, J. W. Lynn, F. Dogan, and I. A. Aksay, Phys. Rev. Lett. **73**, 3459 (1994).
[16] E. M. Forgan and S. L. Lee, Phys. Rev. Lett. **75**, 1422 (1995).
[17] S. T. Johnson *et al.*, Phys. Rev. Lett. **82**, 2792 (1999).
[18] P. G. Kealey *et al.*, Phys. Rev. B **64**, 174501 (2001).
[19] C. Simon, A. Pautrat, G. Poullain, C. Goupil, C. Leblond-Harnois, X. Chaud, and A. Brûlet, Phys. Rev. B **70**, 024502 (2004).
[20] T. Klein, I. Joumard, S. Blanchard, J. Marcus, R. Cubitt, T. Giamarchi, and P. Le Doussal, Nature (London) **413**, 404 (2001).
[21] U. Divakar *et al.*, Phys. Rev. Lett. **92**, 237004 (2004).
[22] M. Laver, E. M. Forgan, A. B. Abrahamsen, C. Bowell, T. Geue, and R. Cubitt, Phys. Rev. Lett. **100**, 107001 (2008).
[23] L. DeBeer-Schmitt, M. R. Eskildsen, M. Ichioka, K. Machida, N. Jenkins, C. D. Dewhurst, A. B. Abrahamsen, S. L. Bud'ko, and P. C. Canfield, Phys. Rev. Lett. **99**, 167001 (2007).
[24] P. G. Kealey *et al.*, Phys. Rev. Lett. **84**, 6094 (2000).
[25] A. D. Bianchi *et al.*, Science **319**, 177 (2008).
[26] R. Gilardi *et al.*, Phys. Rev. Lett. **88**, 217003 (2002).
[27] R. Gilardi, J. Mesot, S. P. Brown, E. M. Forgan, A. Drew, S. L. Lee, R. Cubitt, C. D. Dewhurst, T. Uefuji, and K. Yamada, Phys. Rev. Lett. **93**, 217001 (2004).
[28] S. P. Brown, D. Charalambous, E. C. Jones, E. M. Forgan, P. G. Kealey, A. Erb, and J. Kohlbrecher, Phys. Rev. Lett. **92**, 067004 (2004).
[29] P. I. Soininen, C. Kallin, and A. J. Berlinsky, Phys. Rev. B **50**, 13883 (1994).
[30] Y. Ren, J.-H. Xu, and C. S. Ting, Phys. Rev. Lett. **74**, 3680 (1995).
[31] J.-H. Xu, Y. Ren, and C.-S. Ting, Phys. Rev. B **53**, R2991 (1996).
[32] A. J. Berlinsky, A. L. Fetter, M. Franz, C. Kallin, and P. I. Soininen, Phys. Rev. Lett. **75**, 2200 (1995).
[33] M. Franz, C. Kallin, P. I. Soininen, A. J. Berlinsky, and A. L. Fetter, Phys. Rev. B **53**, 5795 (1996).
[34] M. Ichioka, N. Enomoto, N. Hayashi, and K. Machida, Phys. Rev. B **53**, 2233 (1996).
[35] M. Ichioka, N. Hayashi, N. Enomoto, and K. Machida, Phys. Rev. B **53**, 15316 (1996).
[36] I. Affleck, M. Franz, and M. H. Sharifzadeh Amin, Phys. Rev. B **55**, R704 (1997).
[37] N. Enomoto, M. Ichioka, and K. Machida, J. Phys. Soc. Jpn. **66**, 204 (1997).
[38] M. H. S. Amin, I. Affleck, and M. Franz, Phys. Rev. B **58**, 5848 (1998).
[39] M. Ichioka, A. Hasegawa, and K. Machida, Phys. Rev. B **59**, 8902 (1999).
[40] J. Yeo and M. A. Moore, Phys. Rev. Lett. **78**, 4490 (1997).
[41] N. Nakai, P. Miranović, M. Ichioka, and K. Machida, Phys. Rev. Lett. **89**, 237004 (2002).
[42] M. R. Eskildsen, C. D. Dewhurst, B. W. Hoogenboom, C. Petrovic, and P. C. Canfield, Phys. Rev. Lett. **90**, 187001 (2003).
[43] A. Erb, E. Walker, and R. Flükiger, Physica C **258**, 9 (1996).
[44] M. Roulin, A. Junod, A. Erb, and E. Walker, Phys. Rev. Lett. **80**, 1722 (1998).
[45] L. J. Campbell, M. M. Doria, and V. G. Kogan, Phys. Rev. B **38**, 2439 (1988).
[46] R. Cubitt, E. M. Forgan, D. McK. Paul, S. L. Lee, J. S. Abell, H. Mook, and P. A. Timmins, Physica B **180-181**, 377 (1992).
[47] P. Harris, B. Lebech, and J. S. Pedersen, J. Appl. Crystallogr. **28**, 209 (1995).
[48] V. G. Kogan, Phys. Rev. B **24**, 1572 (1981).
[49] S. L. Thiemann, Z. Radović, and V. G. Kogan, Phys. Rev. B **39**, 11406 (1989).
[50] M. B. Walker and T. Timusk, Phys. Rev. B **52**, 97 (1995).
[51] D. K. Christen, F. Tasset, S. Spooner, and H. A. Mook, Phys. Rev. B **15**, 4506 (1977).
[52] A. Yaouanc, P. Dalmas de Réotier, and E. H. Brandt, Phys. Rev. B **55**, 11107 (1997).
[53] L. I. Burlachkov, Europhys. Lett. **8**, 673 (1989).
[54] M. Franz, I. Affleck, and M. H. S. Amin, Phys. Rev. Lett. **79**, 1555 (1997).
[55] G. Eilenberger, Z. Phys. **214**, 195 (1968).
[56] M. C. Schabel, C.-H. Park, A. Matsuura, Z.-X. Shen, D. A. Bonn, X. Liang, and W. N. Hardy, Phys. Rev. B **57**, 6090 (1998).
[57] M. C. Schabel, C.-H. Park, A. Matsuura, Z.-X. Shen, D. A. Bonn, R. Liang, and W. N. Hardy, Phys. Rev. B **57**, 6107 (1998).
[58] In anisotropic London theory, the degeneracy that exists in VL orientations is broken when the field is applied at an angle to a principal crystal axis, e.g., the *c* axis. In the uniaxial case, anisotropic London theory predicts (Ref. 45) that the vortex nearest-neighbor direction should lie along the direction of shortest penetration depth, which in this case would be the horizontal direction because the rotation is about the vertical axis. The electromagnetic interaction that favors this orientation arises from the coupling (caused by the rotation) of the effective mass in the horizontal direction to the effective mass along the *c* axis. In the present case, the small rotation of 10° makes a negligible change in the penetration depth in the horizontal direction and hence the distortion of the VL from regular hexagonal is still dominated by the basal-plane anisotropy. Nevertheless, the coupling breaks the degeneracy of VL orientations and therefore would give rise to a preferential orientation independent of the basal-plane anisotropy.